

# The Dark Energy Equation of State using Alternative Cosmic High- $z$ Tracers

M. Plionis<sup>1,2</sup>, R. Terlevich<sup>2</sup>, S. Basilakos<sup>3</sup>, F. Bresolin<sup>4</sup>, E. Terlevich<sup>2</sup>,  
J. Melnick<sup>5</sup>, R. Chavez<sup>2</sup>

<sup>1</sup> Institute of Astronomy & Astrophysics, National Observatory of Athens, Palaia Penteli 152 36, Athens, Greece.

<sup>2</sup> Instituto Nacional de Astrofísica Óptica y Electrónica, AP 51 y 216, 72000, Puebla, México.

<sup>3</sup> Academy of Athens, Research Center for Astronomy and Applied Mathematics, Soranou Efessiou 4, 11527, Athens, Greece

<sup>4</sup> Institute for Astronomy of the University of Hawaii, 2680 Woodlawn Drive, 96822 Honolulu, HI USA

<sup>5</sup> European Southern Observatory, Alonso de Cordova 3107, Santiago, Chile

E-mail: mplionis@astro.noa.gr

**Abstract.** We propose to use alternative cosmic tracers to measure the dark energy equation of state and the matter content of the Universe [ $w(z)$  &  $\Omega_m$ ]. Our proposed method consists of two components: (a) tracing the Hubble relation using HII galaxies which can be detected up to very large redshifts,  $z \sim 4$ , as an alternative to supernovae type Ia, and (b) measuring the clustering pattern of X-ray selected AGN at a median redshift of  $\sim 1$ . Each component of the method can in itself provide interesting constraints on the cosmological parameters, especially under our anticipation that we will reduce the corresponding random and systematic errors significantly. However, by joining their likelihood functions we will be able to put stringent cosmological constraints and break the known degeneracies between the *dark energy* equation of state (whether it is constant or variable) and the matter content of the universe and provide a powerful and alternative route to measure the contribution to the global dynamics and the equation of state of *dark energy*. A preliminary joint analysis of X-ray selected AGN clustering (based on the largest to-date XMM survey; the 2XMM) and the currently largest SNIa sample, the *Constitution* set (Hicken et al.), using as priors a flat universe and the WMAP5 normalization of the power-spectrum, provides:  $\Omega_m = 0.27 \pm 0.02$  and  $w = -0.96 \pm 0.07$ . Equivalent and consistent results are provided by the joint analysis of X-ray selected AGN clustering and the latest Baryonic Acoustic Oscillation measures, providing:  $\Omega_m = 0.27 \pm 0.02$  and  $w = -0.97 \pm 0.04$ .

## 1. Introduction

We live in a very exciting period for our understanding of the Cosmos. Over the past decade the accumulation and detailed analyses of high quality cosmological data (eg., supernovae type Ia, CMB temperature fluctuations, galaxy clustering, high- $z$  clusters of galaxies, etc.) have strongly suggested that we live in a flat and accelerating universe, which contains at least some sort of cold dark matter to explain the clustering of extragalactic sources, and an extra component which acts as having a negative pressure, as for example the energy of the vacuum (or in a more general setting the so called *dark energy*), to explain the observed accelerated cosmic expansion (eg. Riess, et al. 1998; 2004; 2007, Perlmutter et al. 1999; Spergel et al. 2003, 2007, Tonry et al. 2003; Schuecker et al. 2003; Tegmark et al. 2004; Seljak et al. 2004; Allen et al. 2004;

Basilakos & Plionis 2005; 2006; 2009; Blake et al. 2007; Wood-Vasey et al. 2007, Davis et al. 2007; Kowalski et al. 2008, Komatsu et al. 2008; Hicken et al. 2009, etc).

Due to the absence of a well-motivated fundamental theory, there have been many theoretical speculations regarding the nature of the exotic *dark energy*, on whether it is a cosmological constant, a scalar or vector fields which provide a time varying dark-energy equation of state, usually parametrized by:

$$p_Q = w(z)\rho_Q , \quad (1)$$

with  $p_Q$  and  $\rho_Q$  the pressure and density of the exotic dark energy fluid and

$$w(z) = w_0 + w_1 f(z) , \quad (2)$$

with  $w_0 = w(0)$  and  $f(z)$  an increasing function of redshift [ eg.,  $f(z) = z/(1+z)$ ] (see Peebles & Ratra 2003 and references therein, Chevalier & Polarski 2001, Linder 2003, Dicus & Repko 2004; Wang & Mukherjee 2006). Of course, the equation of state could be such that  $w$  does not evolve cosmologically.

Two very extensive recent reports have identified *dark energy* as a top priority for future research: "Report of the Dark Energy Task Force (advising DOE, NASA and NSF) by Albrecht et al. (2006), and "Report of the ESA/ESO Working Group on Fundamental Cosmology", by Peacock et al. (2006). It is clear that one of the most important questions in Cosmology and cosmic structure formation is related to the nature of *dark energy* (as well as whether it is the sole interpretation of the observed accelerated expansion of the Universe) and its interpretation within a fundamental physical theory. To this end a large number of very expensive experiments are planned and are at various stages of development, among which the *Dark Energy Survey* (DES: <http://www.darkenergysurvey.org/>), the *Joint Dark Energy Mission* (JDEM: <http://jdem.gsfc.nasa.gov/>), *HETDEX* (<http://www.as.utexas.edu/hetdex/>), Pan-STARRS: <http://pan-starrs.ifa.hawaii.edu>, etc.

Therefore, the paramount importance of the detection and quantification of *dark energy* for our understanding of the cosmos and for fundamental theories implies that the results of the different experiments should not only be scrutinized, but alternative, even higher-risk, methods to measure *dark energy* should be developed and applied as well. It is within this paradigm that our current work falls. Indeed, we wish to constrain the *dark energy* equation of state using, individually and in combination, the Hubble relation and large-scale structure (clustering) methods, but utilizing alternative cosmic tracers for both of these components.

From one side we wish to trace the Hubble function using HII galaxies, which can be observed at higher redshifts than those sampled by current SNIa surveys and thus at distances where the Hubble function is more sensitive to the cosmological parameters. The HII galaxies can be used as standard candles (Melnick, Terlevich & Terlevich 2000, Melnick 2003; Siegel et al. 2005; Plionis et al. 2009) due to the correlation between their velocity dispersion, metallicity and  $H_\beta$  luminosity (Melnick 1978, Terlevich & Melnick 1981, Melnick, Terlevich & Moles 1988), once we reduce significantly their distance modulus uncertainties, which at present are unacceptably large for precision cosmology ( $\sigma_\mu \simeq 0.52$  mag; Melnick, Terlevich & Terlevich 2000). Furthermore, the use of such an alternative high- $z$  tracer will enable us to check the SNIa based results and lift any doubts that arise from the fact that they are the only tracers of the Hubble relation used to-date (for possible usage of GRBs see for example, Ghirlanda et al. 2006; Basilakos & Perivolaropoulos 2008)<sup>1</sup>.

<sup>1</sup> GRBs appear to be anything but standard candles, having a very wide range of isotropic equivalent luminosities and energy outputs. Nevertheless, correlations between various properties of the prompt emission and in some cases also the afterglow emission have been used to determine their distances. A serious problem that hampers a straight forward use of GRBs as Cosmological probes is the intrinsic faintness of the nearby events, a fact which introduces a bias towards low (or high) values of GRB observables and therefore the extrapolation of their

From the other side we wish to use X-ray selected AGN at a median redshift of  $\sim 1$ , which is roughly the peak of their redshift distribution (see Basilakos et al. 2004; 2005, Miyaji et al. 2007), in order to determine their clustering pattern and compare it with that predicted by different cosmological models.

Although each of the previously discussed components of our project (Hubble relation using HII galaxies and angular/spatial clustering of X-ray AGN) will provide interesting and relatively stringent constraints on the cosmological parameters, especially under our anticipation that we will reduce significantly the corresponding random and systematic errors, it is the combined likelihood of these two type of analyses that enables us to break the known degeneracies between cosmological parameters and determine with great accuracy the *dark energy* equation of state (see Basilakos & Plionis 2005; 2006; 2009).

Below we present the basic methodology of each of the two main components of our proposal, necessary in order to constrain the *dark energy* equation of state.

## 2. Cosmological Parameters from the Hubble Relation

It is well known that in the matter dominated epoch and in flat universes, the Hubble relation depends on the cosmological parameters via the following equation:

$$H(z) = H_0 E(z) \quad \text{with} \quad E(z) = \left[ \Omega_m (1+z)^3 + \Omega_Q \exp \left( 3 \int_0^z \frac{1+w(x)}{1+x} dx \right) \right]^{\frac{1}{2}}, \quad (3)$$

which is simply derived from Friedman's equation. We remind the reader that  $\Omega_m$  and  $\Omega_Q (\equiv 1 - \Omega_m)$  are the present fractional contributions to the total cosmic mass-energy density of the matter and dark energy source terms, respectively.

Supernovae SNIa are considered standard candles at peak luminosity and therefore they have been used not only to determine the Hubble constant (at relatively low redshifts) but also to trace the curvature of the Hubble relation at high redshifts (see Riess et al. 1998, 2004, 2007; Perlmutter et al. 1998, 1999; Tonry et al. 2003; Astier et al. 2006; Wood-Vasey et al. 2007; Davis et al. 2007; Kowalski et al 2008; Hicken et al. 2009). Practically one relates the distance modulus of the SNIa to its luminosity distance,  $d_L$ , through which the cosmological parameters enter:

$$\mu = m - M = 5 \log d_L + 25 \quad \text{where} \quad d_L = (1+z) \frac{c}{H_0} \int_0^z \frac{dz}{E(z)}. \quad (4)$$

The main result of numerous studies using this procedure is that distant SNIa's are dimmer on average by  $\sim 0.2$  mag than what expected in an Einstein-deSitter model, which translates in them being  $\sim 10\%$  further away than expected.

The amazing consequence of these results is that we live in an accelerating phase of the expansion of the Universe, an assertion that needs to be scrutinized on all possible levels, one of which is to verify the accelerated expansion of the Universe using alternative to SNIa's extragalactic standard candles. Furthermore, the cause and rate of the acceleration is of paramount importance, ie., the *dark energy* equation of state is the next fundamental item to search for and to these directions we hope to contribute with our current project.

### 2.1. Theoretical Expectations:

To appreciate the magnitude of the Hubble relation variations due to the different *dark energy* equations of state, we plot in Figure 1 the relative deviations of the distance modulus,  $\Delta\mu$ , of

correlations to low- $z$  events is faced with serious problems. One might also expect a significant evolution of the intrinsic properties of GRBs with redshift (also between intermediate and high redshifts) which can be hard to disentangle from cosmological effects. Finally, even if a reliable scaling relation can be identified and used, the scatter in the resulting luminosity and thus distance modulus is still fairly large.

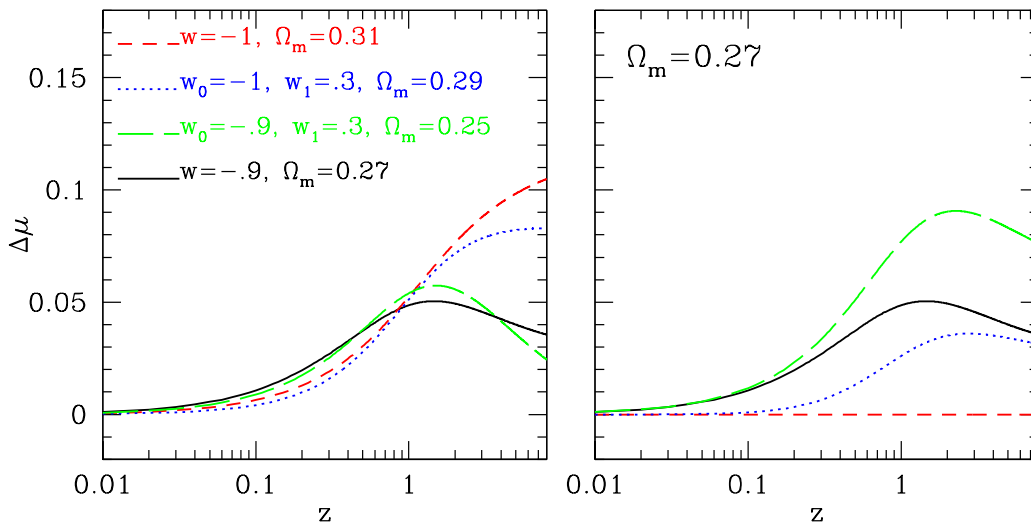


**Figure 1.** *Left Panel:* The expected distance modulus difference between the *dark-energy* models shown and the reference  $\Lambda$ -model ( $w = -1$ ) with  $\Omega_m = 0.27$ . *Right Panel:* The expected distance modulus differences once the  $\Omega_m$ - $w(z)$  degeneracy is broken (imposing the same  $\Omega_m$  value as in the comparison model).

different *dark-energy* models from a nominal *standard* ( $w = -1$ )  $\Lambda$ -cosmology (with  $\Omega_m = 0.27$  and  $\Omega_\Lambda = 0.73$ ), with the relative deviations defined as:

$$\Delta\mu = \mu_\Lambda - \mu_{\text{model}}. \quad (5)$$

The parameters of the different models used are shown in Figure 1. As far as the *dark-energy* equation of state parameter is concerned, we present the deviations from the *standard* model of two models with a constant  $w$  value and of two models with an evolving equation of state parameter, utilizing the form of eq.(2). In the left panel of Figure 1 we present results for selected values of  $\Omega_m$ , while in the right panel we use the same *dark-energy* equations of state parameters but for the same value of  $\Omega_m (= 0.27)$  (ie., we eliminate the  $\Omega_m - w(z)$  degeneracy).

Three important observations should be made from Figure 1:

- (i) The relative magnitude deviations between the different *dark-energy* models are quite small (typically  $\lesssim 0.1$  mag), which puts severe pressure on the necessary photometric accuracy of the relevant observations.
- (ii) The largest relative deviations of the distance moduli occur at redshifts  $z \gtrsim 1.5$ , and thus at quite larger redshifts than those currently traced by SN Ia samples, and
- (iii) There are strong degeneracies between the different cosmological models at redshifts  $z \lesssim 1$ , but in some occasions even up to much higher redshifts (one such example is shown in Figure 1 between the models with  $(\Omega_m, w_0, w_1) = (0.31, -1, 0)$  and  $(0.29, -1, 0.3)$ ).

Luckily, such degeneracies can be broken, as discussed already in the introduction, by using other cosmological tests (eg. the clustering of extragalactic sources, the CMB shift parameter, BAO's, etc). Indeed, current evidence overwhelmingly show that the total matter content of the universe is within the range:  $0.2 \lesssim \Omega_m \lesssim 0.3$ , a fact that reduces significantly the degeneracies between the cosmological parameters.

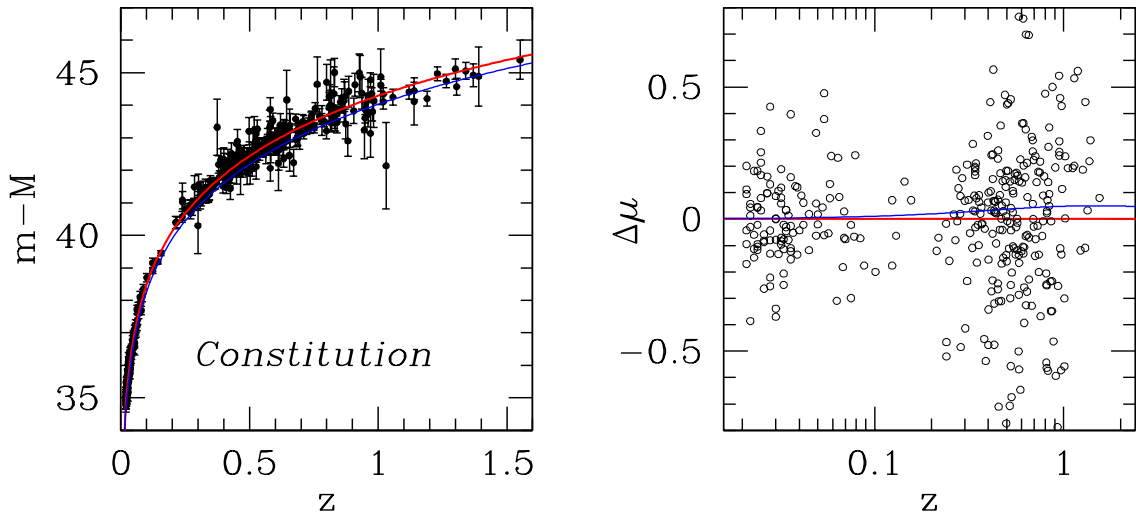


**Figure 2.** *Left Panel:* SNIa distance moduli as a function of redshift. *Right Panel:* Distance moduli difference between the  $\Lambda$ -model and the SNIa data. The blue line is the corresponding difference between the reference ( $w = -1$ ) and the  $w = -0.85$  *dark-energy* models.

## 2.2. Larger numbers or higher redshifts ?

In order to define an efficient strategy to put stringent constraints on the *dark-energy* equation of state, we have decided to re-analyse two recently compiled SNIa samples, the Davis et al. (2007) [hereafter *D07*] compilation of 192 SNIa (based on data from Wood-Vasey et al. 2007, Riess et al. 2007 and Astier et al. 2007) and the *Constitution* compilation of 397 SNIa (Hicken et al. 2009). Note that the two samples are not independent since most of the *D07* is included in the *Constitution* sample.

Firstly, we present in the left panel of Figure 2 the *Constitution* SNIa distance moduli overplotted (red-line) with the theoretical expectation of a flat cosmology with  $(\Omega_m, w) = (0.27, -1)$ . In the right panel we plot the distance moduli difference between the SNIa data and the previously mentioned model. To appreciate the level of accuracy needed in order to put constraints on the equation of state parameter, we also plot the distance moduli difference between the reference  $(\Omega_m, w) = (0.27, -1)$  and the  $(\Omega_m, w) = (0.27, -0.85)$  models (thin blue line).

We proceed to analyse the SNIa data by defining the usual likelihood estimator<sup>2</sup> as:

$$\mathcal{L}^{\text{SNIa}}(\mathbf{p}) \propto \exp[-\chi_{\text{SNIa}}^2(\mathbf{p})/2] \quad (6)$$

where  $\mathbf{p}$  is a vector containing the cosmological parameters that we want to fit for, and

$$\chi_{\text{SNIa}}^2(\mathbf{p}) = \sum_{i=1}^N \left[ \frac{\mu^{\text{th}}(z_i, \mathbf{p}) - \mu^{\text{obs}}(z_i)}{\sigma_i} \right]^2, \quad (7)$$

where  $\mu^{\text{th}}$  is given by eq.(3),  $z_i$  is the observed redshift and  $\sigma_i$  the observed distance modulus uncertainty. Here we will constrain our analysis within the framework of a flat ( $\Omega_{\text{tot}} = 1$ ) cosmology and therefore the corresponding vector  $\mathbf{p}$  is:  $\mathbf{p} \equiv (\Omega_m, w_0, w_1)$ . We will use only SNIa with  $z > 0.02$  in order to avoid redshift uncertainties due to the local bulk flow (eg. Hudson et al. 1999 and references therein).

<sup>2</sup> Likelihoods are normalized to their maximum values.

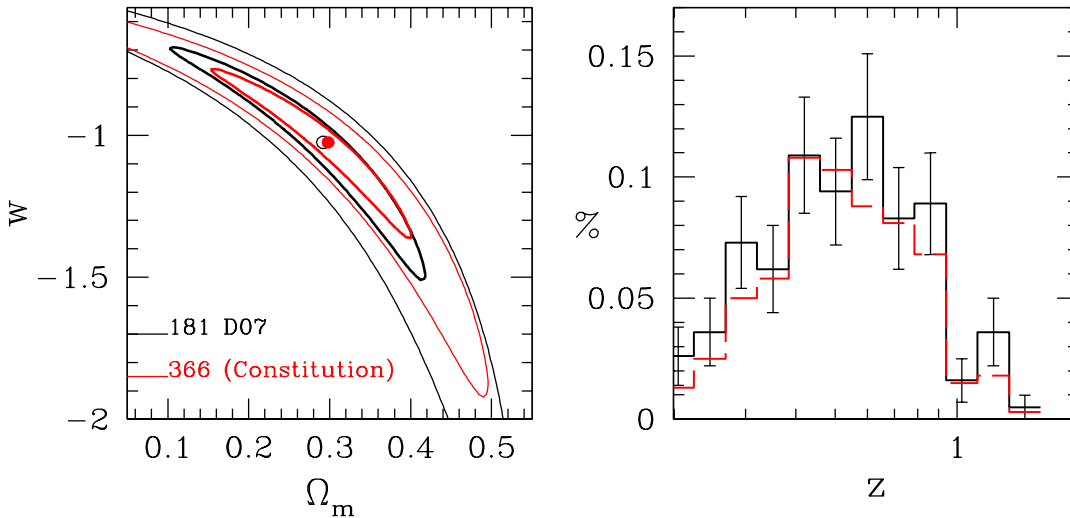


**Figure 3.** *Left panel:* Cosmological parameter solution space using either of the two SNIa data sets (*Constitution*: red contours and *D07*: black contours). Contours corresponding to the 1 and 3 $\sigma$  confidence levels are shown (ie., plotted where  $-2\ln\mathcal{L}/\mathcal{L}_{\max}$  is equal to 2.30 and 11.83, respectively). *Right Panel:* Normalized redshift distributions of the two SNIa data sets.

*2.2.1. Larger Numbers?* The first issue that we wish to address is how better have we done in imposing cosmological constraints by increasing the available SNIa sample from 181 to 366, ie., increasing the sample by more than 100%. In Table 1 we present various solutions using each of the two previously mentioned samples. Note that since only the relative distances of the SNIa are accurate and not their absolute local calibration, we always marginalize with respect to the internally derived Hubble constant (note that fitting procedures exist which do not need to *a priori* marginalize over the internally estimated Hubble constant; eg., Wei 2008). Although the derived cosmological parameters are consistent between the two data sets, possibly indicating the robustness of the method, the corresponding goodness of fit (the reduced  $\chi^2$ ) is significantly larger in the case of the *Constitution* set (1.21 compared to 1.045 of the *D07* set). This appears to be the outcome of the different approaches chosen in order to join the different contributing SNIa sets. According to Hicken 2009 (private communication) in the case of the *D07* the nearby SNIa were imposed to provide a  $\chi^2/df \simeq 1$  by hand, while no such fine-tuning was imposed on the UNION set (on which the *Constitution* set is based). A secondary reason could be that the latter set includes distant SNIa which have typically larger distance modulus uncertainties, with respect to those used in *D07*. Overall, the higher  $\chi^2/df$  value of the *Constitution* set should be attributed to a typically lower uncertainty in  $\mu$ . As a crude test, we have increased by 20% the distance modulus uncertainty of the *Constitution* nearby SNIa ( $z \lesssim 0.4$ ) and indeed we obtain  $\chi^2/df \simeq 1.07$ , similar to that of *D07*.

In Figure 3 we can also see that although the SNIa sample has doubled in size, the well-known *banana* shape region of the  $(\Omega_m, w)$  solution space, indicating the degeneracy between the two cosmological parameters, is reproduced by both data sets. However, there is a reduction of the size of the solution space when using the *Constitution* SNIa compilation (see also Table 1), and at roughly the level expected from Poisson statistics.

A first conclusion is therefore that *the increase by  $\sim 100\%$  of the Constitution sample has not provided significantly more stringent constraints to the cosmological parameters.* We have verified that the larger number of SNIa's in the *Constitution* sample are not preferentially



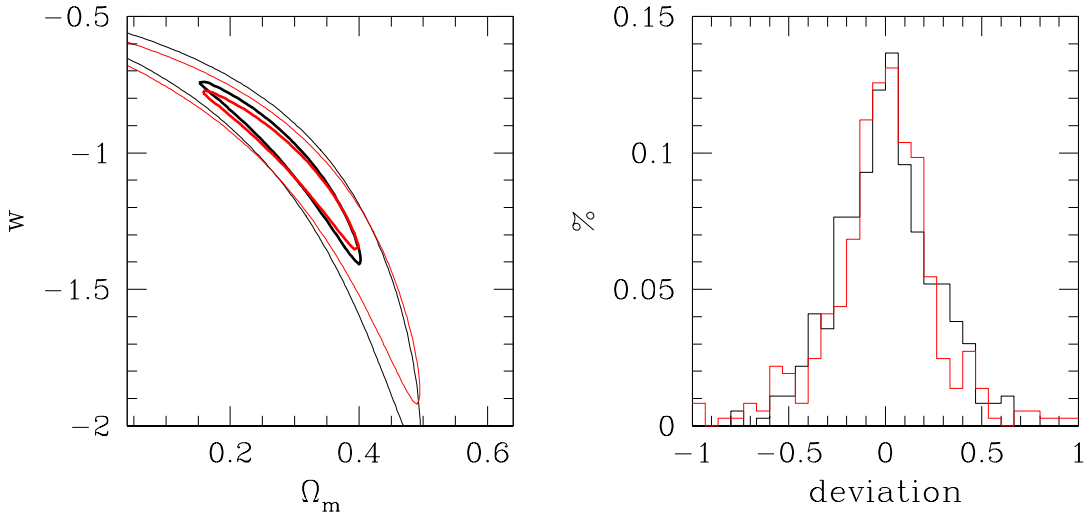


**Figure 4.** *Left Panel:* Comparison between the *Constitution* SNIa constraints (red contours) and those derived by a Monte-Carlo procedure designed to closely reproduce them (for clarity we show only contours corresponding to 1 and 3  $\sigma$  confidence levels). *Right Panel:* The *Constitution* SNIa distance modulus deviations from the best fit model  $(\Omega_m, w) \simeq (0.30, -1.01)$ ; see Table 1 - and a random realization of the model deviations (red histogram).

**Table 1.** Cosmological parameter fits using the SNIa data within flat cosmologies. Note that for the case where  $\mathbf{p} = (\Omega_m, w)$  (ie., last row), the errors shown are estimated after marginalizing with respect to the other fitted parameter.

<i>D07</i>			<i>Constitution</i>		
w	$\Omega_m$	$\chi^2_{\min}/\text{df}$	w	$\Omega_m$	$\chi^2_{\min}/\text{df}$
-1	$0.280^{+0.025}_{-0.015}$	187.03/180	-1	$0.286^{+0.012}_{-0.018}$	439.78/365
$-1.025^{+0.060}_{-0.045}$	$0.292 \pm 0.018$	187.02/179	$-1.025 \pm 0.030$	$0.298 \pm 0.012$	439.79/364

located at low- $z$ 's (see right panel of Fig.2) - in which case we should have not expected more stringent cosmological constraints using the latter SNIa sample, but rather have a very similar  $z$ -distribution.

We already have a strong hint, from the previously presented comparison between the *D07* and *Constitution* results, that increasing the number of Hubble relation tracers, covering the same redshift range and with the current level of uncertainties as the available SNIa samples, does not appear to be an effective avenue for providing further constraints of the cosmological parameters.

**2.2.2. Lower uncertainties or higher- $z$ 's:** We now resort to a Monte-Carlo procedure which will help us investigate which of the following two directions, which bracket many different possibilities, would provide more stringent cosmological constraints:

- Reduce significantly the distance modulus uncertainties of SNIa, tracing however the same redshift range as the currently available samples, or
- use tracers of the Hubble relation located at redshifts where the models show their largest relative differences ( $z \gtrsim 2$ ), with distance modulus uncertainties comparable to that of the highest redshift SNIa's ( $\langle \sigma_\mu \rangle \simeq 0.4$ )

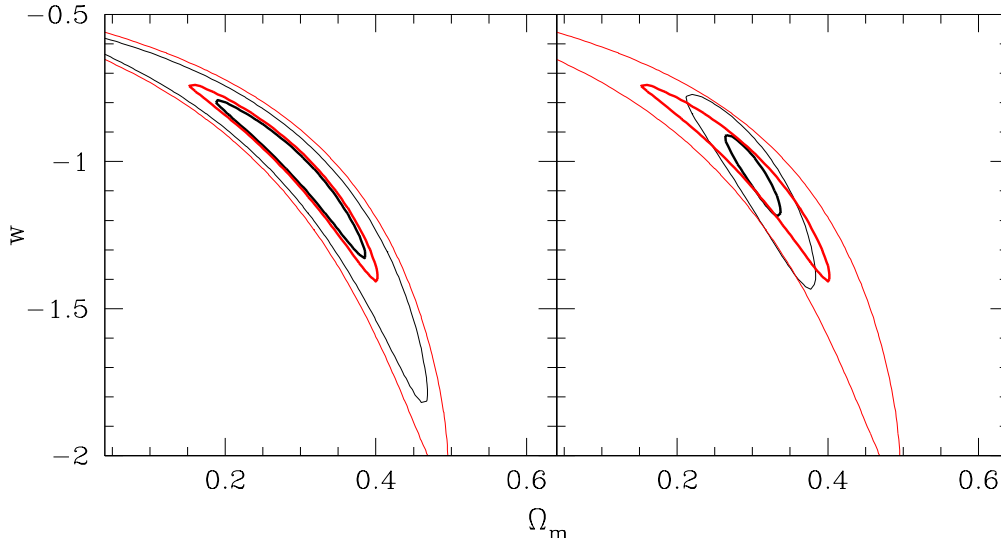


**Figure 5.** Comparison of the model *Constitution* SNIa constraints (red contours) with those derived by reducing to half their uncertainties (*left panel*, and with those derived by adding a sample of 82 high- $z$  tracers ( $2.7 \lesssim z \lesssim 3.5$ ) with a distance modulus mean uncertainty of  $\sigma_\mu \simeq 0.38$  (*right panel*). For clarity we show only contours corresponding to the 1 and 3  $\sigma$  confidence levels.

The Monte-Carlo procedure is based on using the observed high- $z$  SNIa distance modulus uncertainty distribution ( $\sigma_\mu$ ) and a model to assign random  $\mu$ -deviations from a reference  $H(z)$  function, that reproduces exactly the original banana-shaped contours of the  $(\Omega_m, w)$  solution space of Figure 3 (left panel). Indeed, after a trial and error procedure we have found that by assigning to each SNIa (using their true redshift) a distance modulus deviation ( $\delta\mu$ ) from a reference model having a Gaussian distribution with zero mean and variance given by the observed  $\langle \sigma_\mu \rangle^2$ , and using as the relevant individual distance modulus uncertainty the following:  $\sigma_i^2 = \sqrt{(1.2\delta\mu_i)^2 + \phi^2}$  (with  $\phi$  a random Poisson deviate within  $[-0.01, 0.01]$ ) we reproduce exactly the banana-shaped solution range of the reference model. This can be seen clearly in the upper left panel of Figure 4, where we plot the original *Constitution* SNIa solution space (red contours) and the model solution space (black contours). In the right panel we show the distribution of the true SNIa deviations from the best fitted model as well as a random realization of the model deviations.

Armed with the above procedure we can now address the questions posed previously. Firstly, we reduce to half the random deviations of the SNIa distance moduli from the reference model (with the corresponding reduction of the relevant uncertainty,  $\sigma_i$ ). The results of the likelihood analysis can be seen in the left panel of Figure 5. There is a reduction of the range of the solution space, but indeed quite a small one. Secondly, we add to the *Constitution* SNIa sample, a mock high- $z$  subsample of 82 objects constructed as follows: For each  $z > 0.68$  SNIa we add one mock SNIa having as a redshift  $z + \delta z$  where  $\delta z = 2$  and the same distance modulus uncertainty. Note that these new 82 SNIa are distributed between  $2.68 \lesssim z \lesssim 3.55$ , ie., in a range where the largest deviations between the different cosmological models occur (see Figure 1). The deviations from the reference model of these additional SNIa are based on their original  $\mu$  uncertainty distribution (ie., we have assumed that the new high- $z$  tracers will have similar uncertainties as their  $z \gtrsim 0.68$  counterparts, which on average is  $\langle \sigma_\mu \rangle \simeq 0.38$ ). We now find a significantly reduced solution space (right panel of Figure 5), which shows that indeed by increasing the  $H(z)$  tracers by a few tens, at those redshifts where the largest deviations between models occur, can have a significant impact on the recovered cosmological parameter solution space. Similarly, if we use a reference



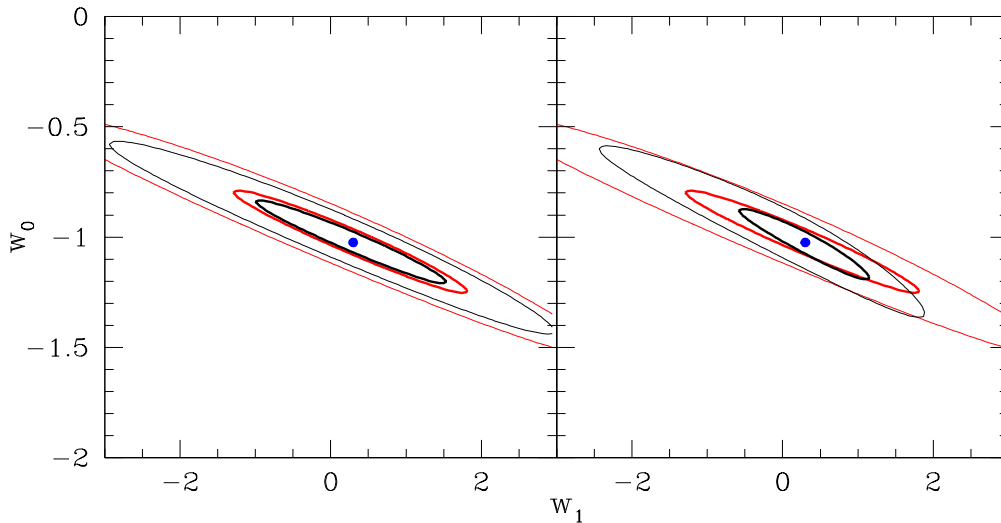


**Figure 6.** Similar as in Figure 5, but allowing for an evolving DE equation of state according to eq. (2) and after marginalizing with respect to  $\Omega_m$ . The input cosmological model has  $(w_0, w_1) = (-1.025, 0.3)$  and is represented by the red contours. Again we show for clarity only contours corresponding to the 1 and 3  $\sigma$  confidence levels.

model with an evolving dark-energy equation of state (as that of eq. 2), and after marginalizing with respect to  $\Omega_m$ , we also find a significantly larger reduction of the  $(w_0, w_1)$  solution space when we include the high redshift tracer subsample (Fig.6, right panel) with respect to the distance modulus uncertainty reduction (by 1/2) case (Fig. 6, left panel).

The main conclusion of the previous analysis is that a relatively better strategy to decrease the uncertainties of the cosmological parameters, based on the Hubble relation, is to use standard candles which trace also the redshift range  $2 \lesssim z \lesssim 4$ . Below we present one such possibility by suggesting an alternative, to the SNIa standard candles, namely HII galaxies (eg. Melnick 2003; Siegel et al. 2005).

### 2.3. Hubble Relation using HII galaxies

We now reach our suggestion to use an alternative and potentially very powerful technique to estimate cosmological distances, which is the relation between the luminosity of the  $H_\beta$  line and the stellar velocity dispersion, measured from the line-widths, of HII regions and galaxies (Terlevich & Melnick 1981, Melnick, Terlevich & Moles 1988). The cosmological use of this distance indicator has been tested in Melnick, Terlevich & Terlevich (2000) and Siegel et al (2005) (see also the review by Melnick 2003). The presence of O and B-type stars in HII regions causes the strong Balmer line emission, in both  $H_\alpha$  and  $H_\beta$ . Furthermore, the fact that the bolometric luminosities of HII galaxies are dominated by the starburst component implies that their luminosity per unit mass is very large, despite the fact that the galaxies are low-mass. Therefore they can be observed at very large redshifts, and this fact makes them cosmologically very interesting objects. Furthermore, it has been shown that the  $L(H_\beta) - \sigma$  correlation holds at large redshifts (Koo et al. 1996, Pettini et al. 2001, Erb et al. 2003) and therefore it can be used to trace the Hubble relation at cosmologically interesting distances. One of the most important prerequisites in using such relations, as distance estimators, is the accurate determination of their zero-point. To this end, Melnick et al (1988) used giant HII regions in nearby late-type galaxies and derived the following empirical relation (using a Hubble constant of  $H_0 = 71$  km/sec/Mpc):

$$\log L(H_\beta) = \log M_z + 29.60 \quad \text{with} \quad M_z = \sigma^5 / (O/H) \quad (8)$$

where  $O/H$  is the metallicity. Based on the above relation and the work of Melnick, Terlevich & Terlevich (2000), the distance modulus of HII galaxies can be written as:

$$\mu = 2.5 \log(\sigma^5 / F_{H_\beta}) - 2.5 \log(O/H) - A_{H_\beta} - 26.44, \quad (9)$$

with  $F_{H_\beta}$  and  $A_{H_\beta}$  the flux and extinction in  $H_\beta$ , respectively. The rms dispersion in distance modulus was found to be  $\sim 0.52$  mag. The analysis of Melnick, Terlevich & Terlevich (2000) has shown that most of this dispersion ( $\sim 0.3$  mags) comes from observational errors in the stellar velocity dispersion measurements, from photometric errors and metallicity effects. It is therefore possible to understand and correct the sources of random and systematic errors of the  $L(H_\beta) - \sigma$  relation, and indeed with the availability of new observing techniques and instruments, we hope to reduce significantly the previously quoted rms scatter.

A few words are also due to the possible systematic effects of the above relation. Such effects may be related to the age of the HII galaxy (this can be dealt with by putting a limit in the equivalent width of the  $H_\beta$  line, eg.  $EW(H_\beta) > 25$  Angs; see Melnick 2003), to extinction, to different metallicities and environments. Also the  $EW(H_\beta)$  of HII galaxies at intermediate and high redshifts is smaller than in local galaxies, a fact which should also be taken into account.

We have commenced an investigation of all these effects by using high-resolution spectroscopy of a relatively large number of SDSS low- $z$  HII galaxies, having a range of  $H_\beta$  equivalent widths, luminosities, metal content and local overdensity, in order to understand systematics and reduce the scatter of the HII-galaxy based distance estimator to about half its present value, ie., our target is  $\sim 0.25$  mag. We will also define a medium and high redshift sample (see Pettini et al. 2001; Erb et al. 2003), consisting of a few hundred objects distributed in a range of high-redshifts, which will finally be used to define the high- $z$  Hubble function.

Summarizing, the use of HII galaxies to trace the Hubble relation, as an alternative to the traditionally used SN Ia, is based on the following facts:

- (a) *local and high- $z$  HII galaxies and HII regions are physically very similar systems (Melnick et al 1987) providing a phenomenological relation between the luminosity of the  $H_\beta$  line, the velocity dispersion and their metallicity as traced by  $O/H$  (Melnick, Terlevich & Moles 1988). Therefore HII galaxies can be used as alternative standard candles (Melnick, Terlevich & Terlevich 2000, Melnick 2003; Siegel et al. 2005)*
- (b) *such galaxies can be readily observed at much larger redshifts than those currently probed by SNIa samples, and*
- (c) *it is at such higher redshifts that the differences between the predictions of the different cosmological models appear more vividly.*

Already a sample of 15 such high- $z$  HII galaxies have been used by Siegel et al. (2005) in an attempt to constrain cosmological parameters but the constraints, although in the correct direction, are very weak. We have performed our own re-analysis of this data-set, following however the same procedure as that applied to the SNIa data (ie., we factorize out the internally derived Hubble constant using a fit of the distance moduli in the  $\Omega_m, H_0$  space). The resulting constraints on the  $(\Omega_m, w)$  plane can be seen in Figure 7. We find that  $\Omega_m \lesssim 0.42$  at a 99.99% level, independent of  $w$ . Note that imposing  $w = -1$ , our analysis of the Siegel et al (2005) data set provides  $\Omega_m = 0.19 \pm 0.05$ , which is towards the lower side of the generally accepted values.

Comparing these HII-based results to the present constraints of the latest (*Constitution* SNIa data (right panel of Fig. 7) clearly indicates the necessity to:

- re-estimate carefully the local zero-point of the  $L(H_\beta) - \sigma$  relation,

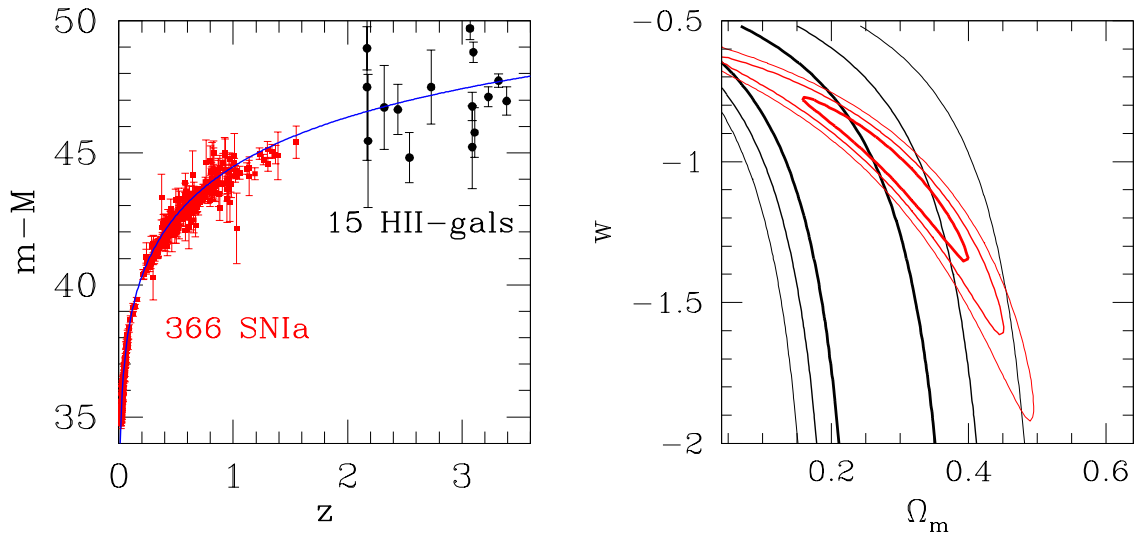


**Figure 7.** *Left Panel:* Distance moduli comparison between the *Constitution* SNIa’s and the 15 high- $z$  HII galaxies of Siegel et al. (2005). *Right Panel:* The corresponding constraints in the  $(\Omega_m, w)$  plane. Although, the HII-galaxy constraints are weak, leaving completely unconstrained the value of  $w$ , they appear to be consistent at a  $\sim 2\sigma$  level with the SNIa results. This plot serves only to indicate the potential of using high- $z$  HII galaxies (once of course we have reduced significantly their distance modulus uncertainties).

- suppress the HII-galaxy distance modulus uncertainties,
- increase the high- $z$  HII galaxy sample by a large fraction,
- make sure to select high- $z$  bona-fide HII-galaxies, excluding those that show indications of rotation (Melnick 2003).

### 3. Cosmological Parameters from the Clustering of X-ray AGN

The method used to put cosmological constraints, based on the angular clustering of some extragalactic mass-tracer (Matsubara 2004, Basilakos & Plionis 2009 and references therein), consists in comparing the observed angular clustering with that predicted by different primordial fluctuations power-spectra, using Limber’s integral equation (Limber 1968) to invert from spatial to angular clustering. By minimizing the differences of the observed and predicted angular correlation function, one can constrain the cosmological parameters that enter in the power-spectrum determination as well as in Limber’s inversion. Using the latter we can relate the angular and spatial clustering of any extragalactic population under the assumption of power-law correlations and the small angle approximation.

#### 3.1. X-ray surveys: Biases and Systematics

X-ray selected AGN provide a relatively unbiased census of the AGN phenomenon, since obscured AGN, largely missed in optical surveys, are included in such surveys. Furthermore, they can be detected out to high redshifts and thus trace the distant density fluctuations providing important constraints on super-massive black hole formation, the relation between AGN activity and Dark Matter (DM) halo hosts, the cosmic evolution of the AGN phenomenon (eg. Mo & White 1996, Sheth et al. 2001), and on cosmological parameters and the dark-energy equation of state (eg. Basilakos & Plionis 2005; 2006).

The earlier ROSAT-based analyses (eg. Boyle & Mo 1993; Vikhlinin & Forman 1995; Carrera et al. 1998; Akylas, Georgantopoulos, Plionis, 2000; Mullis et al. 2004) provided conflicting results on the nature and amplitude of high- $z$  AGN clustering. With the advent of the XMM and *Chandra* X-ray observatories, many groups have attempted to settle this issue, but in vain. Different surveys have provided again a multitude of conflicting results, intensifying the debate (eg. Yang et al. 2003; Manners et al. 2003; Basilakos et al. 2004; Gilli et al. 2005; Basilakos et al. 2005; Yang et al. 2006; Puccetti et al. 2006; Miyaji et al. 2007; Gandhi et al. 2006; Carrera et al. 2007). However, the recent indications of a flux-limit dependent clustering appears to remove most of the above inconsistencies (Plionis et al. 2008).

Furthermore, there are indications for a quite large high- $z$  AGN clustering length, reaching values  $\sim 15 - 18 h^{-1}$  Mpc at the brightest flux-limits (eg., Basilakos et al. 2004; 2005, Puccetti et al. 2006, Plionis et al. 2008), a fact which, if verified, has important consequences for the AGN bias evolution and therefore for the evolution of the AGN phenomenon (eg. Miyaji et al. 2007; Basilakos, Plionis & Ragono-Figueroa 2008). An independent test of these results would be to establish that the environment of high- $z$  AGN is associated with large DM haloes, which being massive should be more clustered (work in progress).

It is also important to understand and overcome the shortcomings and problems that one is facing in order to reliably and unambiguously determine the clustering properties of the X-ray selected AGN. Such a list of problems includes the effects of Cosmic Variance, the so-called amplification bias, the reliability of the  $\log N - \log S$  distribution of the X-ray AGN luminosity function, etc. (see discussion in Plionis et al. 2009).

Recently, Ebrero et al. (2009) derived the angular correlation function of the soft (0.5-2 keV) X-ray sources using 1063 XMM-*Newton* observations at high galactic latitudes. A full description of the data reduction, source detection and flux estimation are presented in Mateos et al. (2008). Note, that the survey contains  $\sim 30000$  point sources within an effective area of  $\sim 125.5$  deg<sup>2</sup> (for  $f_x \geq 1.4 \times 10^{-15}$  erg cm<sup>-2</sup> s<sup>-1</sup>). The details regarding the angular correlation function, the various biases that should be taken into account (the amplification bias and integral constraint), the survey luminosity and selection functions as well as issues related to possible non-AGN contamination, which are estimated to be  $\lesssim 10\%$ , can be found in Ebrero et al (2009).

### 3.2. Details of the Method

An optimal approach to unambiguously determine the clustering pattern of X-ray selected AGN would be to determine both the angular and spatial clustering pattern. The reason being that various systematic effects or uncertainties enter differently in the two types of analyses. On the one side, using  $w(\theta)$  and its Limber inversion, one by-passes the effects of redshift-space distortions and uncertainties related to possible misidentification of the optical counter-parts of X-ray sources. On the other side, using spectroscopic or accurate photometric redshifts to measure  $\xi(r)$  or  $w_p(\theta)$  one by-passes the inherent necessity, in Limber's inversion of  $w(\theta)$ , of the source redshift-selection function (for the determination of which one uses the integrated X-ray source luminosity function, different models of which exist).

The basic integral equation relating the angular and spatial correlation functions is:

$$w(\theta) = 2 \frac{H_0}{c} \int_0^\infty \left( \frac{1}{N} \frac{dN}{dz} \right)^2 E(z) dz \int_0^\infty \xi(r, z) du \quad , \quad (10)$$

where  $dN/dz$  is the source redshift distribution, estimated by integrating the appropriate source luminosity function (in our case that of Ebrero et al. 2009b), folding in also the area curve of the survey. Note that to derive the spatial correlation length from eq. (10), it is necessary to model the spatial correlation function as a power law, assume the small angle approximation as well as a cosmological background model, the latter given by  $E(z)$  (from eq. 3) which for a flat

background and a constant *dark energy* equation of state parameter,  $w$ , reduces to:

$$E(z) = [\Omega_m(1+z)^3 + (1-\Omega_m)(1+z)^{3(1+w)}]^{1/2}. \quad (11)$$

The AGN spatial correlation function is:

$$\xi(r, z) = (1+z)^{-(3+\epsilon)} b^2(z) \xi_{\text{DM}}(r), \quad (12)$$

where  $b(z)$  is the evolution of the linear bias factor (eg. Mo & White 1997; Matarrese et al 1997; Sheth & Tormen 1999; Basilakos & Plionis 2001; 2003, Basilakos et al. 2008 and references therein),  $\epsilon$  is a parameter related to the model of AGN clustering evolution (eg. de Zotti et al. 1990)<sup>3</sup> and  $\xi_{\text{DM}}(r)$  is the corresponding correlation function of the underlying dark matter distribution, given by the Fourier transform of the spatial power spectrum  $P(k)$  of the matter fluctuations, linearly extrapolated to the present epoch:

$$\xi_{\text{DM}}(r) = \frac{1}{2\pi^2} \int_0^\infty k^2 P(k) \frac{\sin(kr)}{kr} dk. \quad (13)$$

The CDM power spectrum is given by:  $P(k) = P_0 k^n T^2(k)$ , with  $T(k)$  the CDM transfer function (Bardeen et al. 1986; Sugiyama 1995) and  $n \simeq 0.96$ , following the 5-year WMAP results (Komatsu et al. 2009), and a baryonic density of  $\Omega_b h^2 = 0.022(\pm 0.002)$ . The normalization of the power-spectrum,  $P_0$ , can be parametrized by the rms mass fluctuations on  $R_8 = 8h^{-1}\text{Mpc}$  scales ( $\sigma_8$ ), according to:

$$P_0 = 2\pi^2 \sigma_8^2 \left[ \int_0^\infty T^2(k) k^{n+2} W^2(kR_8) dk \right]^{-1}, \quad (14)$$

where  $W(kR_8) = 3(\sin kR_8 - kR_8 \cos kR_8)/(kR_8)^3$ . Regarding the Hubble constant we use  $H_0 \simeq 71 \text{ km s}^{-1} \text{ Mpc}^{-1}$  (Freedman 2001; Komatsu et al. 2009). Note, that we also utilize the non-linear corrections introduced by Peacock & Dodds (1994).

We can now compare the observed AGN clustering with the predicted, for different cosmological models, correlation function of the underlying mass,  $\xi_{\text{DM}}(r, z)$ , and thus constrain the cosmological parameters. To this end it is necessary to use a bias evolution model and although a large number of such models have been proposed in the literature, we use here our own approach, which was described initially in Basilakos & Plionis (2001; 2003) and extended in Basilakos, Plionis & Ragone-Figueroa (2008). This bias model is based on linear perturbation theory and the Friedmann-Lemaître solutions of the cosmological field equations, while it also allows for interactions and merging of the mass tracers. Considering that each X-ray AGN is hosted by a dark matter halo, we can analytically predict its bias evolution behavior and conversely by comparing with observations we can determine the mass of the DM halo,  $M_h$ , within which AGN live.

In Figure 8 we show a comparison between our model predictions and observationally based AGN bias results, estimated at the sample's median redshift by:

$$b(\bar{z}) = \left( \frac{r_0}{r_{0,m}} \right)^{\gamma/2} D^{3+\epsilon}(\bar{z}) \quad (15)$$

where  $r_0$  and  $r_{0,m}$  are the measured AGN and the theoretical dark-matter clustering lengths, respectively, while  $D(z)$  is the perturbation's linear growing mode (scaled to unity at the present

<sup>3</sup> Following Kúndic (1997) and Basilakos & Plionis (2005; 2006) we use the constant in comoving coordinates clustering model, ie.,  $\epsilon = -1.2$ .

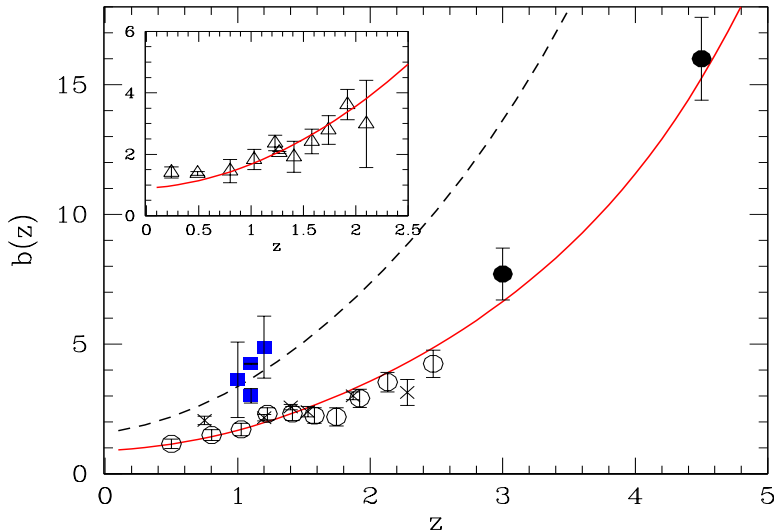


**Figure 8.** The observed evolution of AGN bias compared with the Basilakos et al. (2008) model. Optically selected (SDSS and 2dF) quasars (Croom et al. 2005; Myers et al. 2007; Shen et al. 2007) correspond to circles (empty or filled) points and crosses while soft-band X-ray selected AGN correspond to filled (blue) squares. In the insert we plot the most recent bias values of Ross et al. (2009), based on the SDSS optical quasar uniform sample. The curves reflect our bias evolution model, with the solid (red) lines corresponding to a DM halo mass of  $M \simeq 10^{13} h^{-1} M_{\odot}$  and the dashed lines to  $M \simeq 2.5 \times 10^{13} h^{-1} M_{\odot}$ .

**Table 2.** The best fit values from the likelihood analysis of the X-ray AGN clustering: Errors of the fitted parameters represent  $1\sigma$  uncertainties, while the parameters in bold indicate those fixed during the fitting process.

$\Omega_m$	w	$\sigma_8$	$M_h/10^{13}h^{-1}M_{\odot}$
$0.27 \pm 0.04$	$-0.90^{+0.10}_{-0.16}$	$0.74^{+0.14}_{-0.12}$	$2.50^{+0.50}_{-1.50}$
$0.26 \pm 0.05$	$-0.93^{+0.11}_{-0.19}$	<b>0.8</b>	$2.0^{+0.30}_{-0.2}$
$0.24 \pm 0.06$	<b>-1</b>	$0.83^{+0.11}_{-0.16}$	<b>2.50</b>

time), useful expressions of which can be found for the dark energy models in Silveira & Waga (1994) and in Basilakos (2003).

The preliminary analysis of Basilakos & Plionis (2005; 2006) compared the measured XMM source angular correlation function based on a shallow XMM survey, covering a small solid angle, with the prediction of different spatially flat and constant-w cosmological models. The recent availability, however, of the highly accurate angular correlation function XMM results of Ebrero et al (2009), based on the largest available X-ray AGN sample ( $N \simeq 30000$ ), provided us the means to put stringent constraints on the cosmological parameters (see Basilakos & Plionis 2009). In Table 2 (and in Figure 9) we present the cosmological constraints provided by the current analysis. The power of our procedure can be appreciated by comparing our constraints, under the prior of a flat Universe, with those provided by most other cosmological test (see Fig.2 of Basilakos & Plionis 2009).



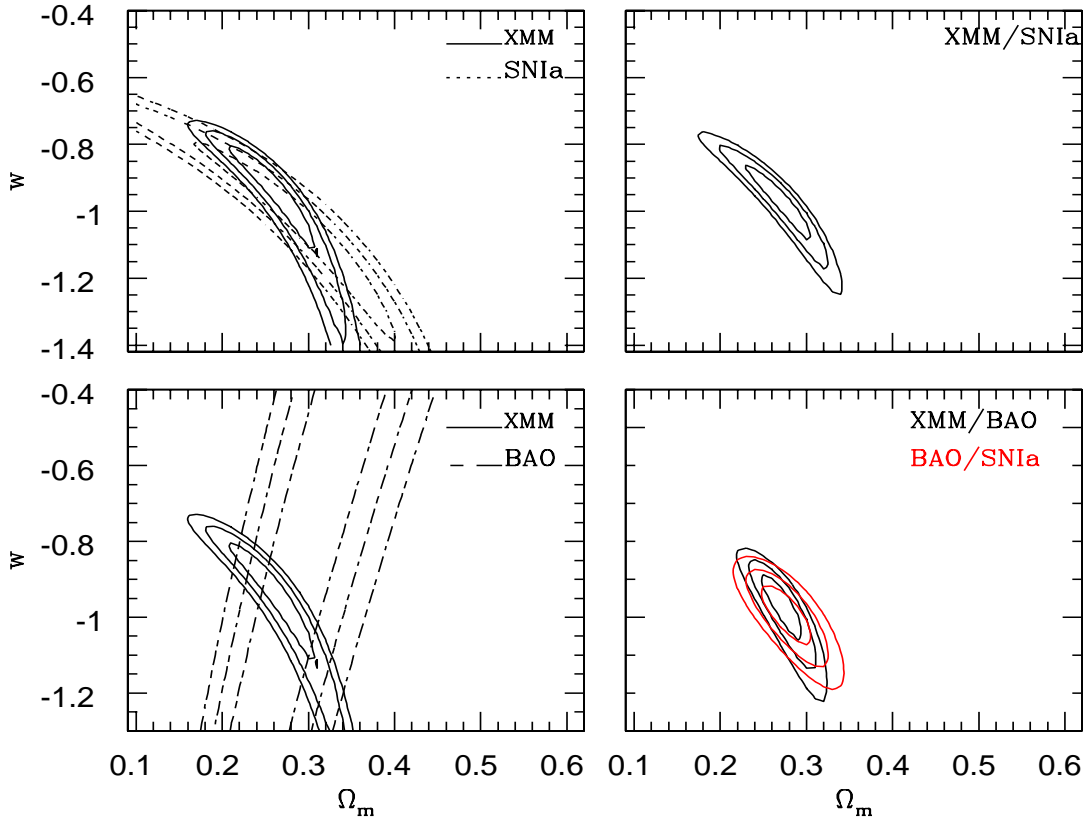


**Figure 9.** *Upper Left Panel:* Likelihood contours on the  $\Omega_m, w$  plane from the X-ray AGN clustering analysis of Basilakos & Plionis (2009) (solid contours) and the *Constitution* SNIa analysis (dashed contours). *Upper Right Panel:* The corresponding joint likelihood contours. *Lower Left Panel:* Likelihood contours from the X-ray AGN clustering analysis and the BAO technique (dashed contours). *Lower Right Panel:* Their corresponding joint likelihood contours (while the BAO-SNIa joint contours are shown in red).

#### 4. Joint Hubble-relation and Clustering analysis

It is evident from Figure 9 (left panels) that with the new X-ray AGN clustering analysis we have been able to reduce significantly the degeneracy between  $w$  and  $\Omega_m$  (see also Table 2). We can further break the degeneracy by adding the constraints provided by either the Hubble relation technique, using here the *Constitution* SNIa sample, or the baryonic acoustic oscillation technique (BAO), which was identified by the U.S. Dark Energy Task Force as one of the four most promising techniques to measure the properties of the *dark energy* and the one less likely to be limited by systematic uncertainties. We remind the reader that BAOs are produced by pressure (acoustic) waves in the photon-baryon plasma in the early universe, generated by dark matter (DM) overdensities. At the recombination era ( $z \sim 1100$ ), photons decouple from baryons and free stream while the pressure wave stalls. Its frozen scale, which constitutes a standard ruler, is equal to the sound horizon length,  $r_s \sim 100 h^{-1}$  Mpc (e.g. Eisenstein, Hu & Tegmark 1998). This appears as a small,  $\sim 10\%$  excess in the galaxy, cluster or AGN power spectrum (and its Fourier transform, the 2-point correlation function) at a scale corresponding to  $r_s$ . First evidences of this excess were recently reported in the clustering of luminous SDSS red-galaxies (Eisenstein et al. 2005, Padmanabhan et al. 2007; Percival et al. 2009).

We therefore perform a joint likelihood analysis, assuming that any two pairs of data sets are

independent (which indeed they are) and thus the joint likelihood can be written as the product of the two individual ones. The current joint likelihood analysis, once we impose  $h = 0.71$  and  $\sigma_8 = 0.8$  (according to Komatsu et al. 2009), provide quite stringent and consistent constraints of the  $\Omega_m$  and  $w$  parameters:

$$\Omega_m = 0.27 \pm 0.02 \quad \text{and} \quad w = -0.96 \pm 0.07 \quad (\text{XMM} - \text{SNIa})$$

$$\Omega_m = 0.27 \pm 0.02 \quad \text{and} \quad w = -0.97 \pm 0.04 \quad (\text{XMM} - \text{BAO})$$

These results can be compared with the more *traditional* joint analysis of the SNIa (*Cosntitution* set in this case) and the BAOs, which provide:

$$\Omega_m = 0.28_{-0.03}^{+0.02} \quad \text{and} \quad w = -0.98 \pm 0.06 \quad (\text{SNIa} - \text{BAO})$$

It is evident that within the errors all the previously presented results are consistent, with the XMM-BAO joint analysis providing the smallest uncertainties of the fitted parameters. This can also be appreciated by inspecting the lower-right panel of Figure 9, which shows that the XMM-BAO joint analysis provides indistinguishable constraints with the corresponding SNIa-BAO analysis.

The necessity, however, to impose constraints on a more general, time-evolving, *dark-energy* equation of state (eq. 3), implies that there is ample space for great improvement and indeed our aim is to complete this project by using a new Hubble relation analysis, based on high- $z$  HII galaxies, as detailed in these proceedings.

#### *Acknowledgments*

We thank Dr J. Ebrero for comments and for providing us with an electronic version of the clustering results and their XMM survey area curve. We also thank Dr. N.P. Ross for providing us an electronic version of the QSO uniform sample bias results. MP also acknowledges financial support under Mexican government CONACyT grant 2005-49878.

#### **References**

- [1] Akylas, A., Georgantopoulos, I., Plionis, M., 2000, MNRAS, 318, 1036
- [2] Albrecht, A., et al., 2006, [astro-ph/0609591](#)
- [3] Allen, S. W., et al., 2004, MNRAS, 353, 457
- [4] Astier, P., et al., 2006, A&A, 447, 31
- [5] Bardeen, J.M., Bond, J.R., Kaiser, N. & Szalay, A.S., 1986, ApJ, 304, 15
- [6] Basilakos, S. & Plionis, M., 2001, ApJ, 550, 522
- [7] Basilakos, S. & Plionis, M., 2003, ApJ, 593, L61
- [8] Basilakos, S., Georgakakis, A., Plionis, M., Georgantopoulos, I., 2004, ApJ, 607, L79
- [9] Basilakos, S., Plionis, M., Georgantopoulos, I., Georgakakis, A., 2005, MNRAS, 356, 183
- [10] Basilakos, S. & Plionis, M., 2005, MNRAS, 360, L35
- [11] Basilakos, S. & Plionis, M., 2006, ApJ, 650, L1
- [12] Basilakos, S., Plionis, M. & Ragone-Figueroa, C., 2008, ApJ, 678, 627
- [13] Basilakos, S. & Perivolaropoulos, L., 2008, MNRAS, 391, 411
- [14] Boyle B.J., Mo H.J., 1993, MNRAS, 260, 925
- [15] Blake, C., et al., 2007, MNRAS, 374, 1527
- [16] Carrera, F.J., et al. 1998, MNRAS, 299, 229
- [17] Carrera, F.J., et al. 2007, A&A, 469, 27
- [18] Chevallier M., & Polarski D., 2001, Int. J. Mod. Phys. D, 10, 213
- [19] Croom, S.M., et al., 2005, MNRAS, 365, 415
- [20] de Zotti, G., et al. 1990, ApJ, 351, 22
- [21] Davis, T.M., et al., 2007, ApJ, 666, 716
- [22] Dicus, D.A. & Repko, W.W., 2004, Phys.Rev.D, 70, 3527,
- [23] Erb, D.K. et al., 2003, ApJ, 591, 101
- [24] Eisenstein, Hu, & Tegmark 1998, ApJ, 504, L57

- [25] Eisenstein et al. 2005, ApJ, 633, 560
- [26] Gandhi, P., et al., 2006, A&A, 457, 393
- [27] Gilli, R., et al. 2003, ApJ, 592, 721
- [28] Ghirlanda, G., Ghisellini, G., Firmani, C., 2006, NewJPhys, 8, 123
- [29] Hudson, M.J., Smith, R.J., Lucey, J.R., Schlegel, D.J., Davies, R.L., 1999, ApJ, 512, L79
- [30] Gilli, R., et al. 2005, A&A, 430, 811
- [31] Kim, M., et al. 2007, ApJ, 659, 29
- [32] Kowalski M. et al., 2008, ApJ, 686, 749
- [33] Kundić, T., 1997, ApJ, 482, 631
- [34] Linder, V. E., 2003, Phys. Rev. Lett., 90, 091301
- [35] Matsubara, T., 2004, ApJ, 615, 573
- [36] Manners, J.C., et al., 2003, MNRAS, 343, 293
- [37] Matarrese, S., Coles, P., Lucchin, F., Moscardini, L., 1997, MNRAS, 286, 115
- [38] Mateos, S., et al., 2008, A&A, 429, 51
- [39] Myers, A.D., Brunner, R.J., Nichol, R.C., Richards, G.T., Schneider D.P., Bahcall, N.A., 2007, ApJ, 658, 85
- [40] Melnick, J., 1978, A&A, 70, 157
- [41] Melnick J., Terlevich, R., Moles, M., 1988, MNRAS, 235, 313;
- [42] Melnick, J., Terlevich, R., Terlevich, E., 2000, MNRAS, 311, 629
- [43] Melnick, J., 2003, *Star Formation Through Time*, ASP Conference Proceedings, 297, Eds E.Perez, et al.
- [44] Miyaji, T., et al., 2007, ApJS, 172, 396
- [45] Mullis C.R., et al., 2004, ApJ, 617, 192
- [46] Mo, H.J, & White, S.D.M 1996, MNRAS, 282, 347
- [47] Padmanabhan et al. 2007, MNRAS, 378, 852
- [48] Peacock et al., 2006, [astro-ph/0610906](#)
- [49] Percival, W.J., et al., 2007, MNRAS, 381, 1053
- [50] Peebles P.J.E., & Ratra, B., 2003, RvMP, 75, 559
- [51] Perlmutter, S., et al., 1998, Nature, 391, 51
- [52] Perlmutter, S., et al., 1999, ApJ, 517, 565
- [53] Pettini, M., et al., 2001, ApJ, 554, 981
- [54] Plionis, M., Rovilos, M., Basilakos, S., Georgantopoulos, I., Bauer, F., 2008, ApJ, 674, L5
- [55] Plionis, M., et al., 2009, JoP, 189, 012032
- [56] Puccetti, S., et al., 2006, A&A, 457, 501
- [57] Riess, A. G., et al., 1998, AJ, 116, 1009
- [58] Riess, A. G., et al., 2004, ApJ, 607, 665
- [59] Riess A.G., 2007, ApJ, 659, 98
- [60] Ross N.P., et al., 2009, ApJ, 697, 1634
- [61] Seljak, U., et al., 2004, Phys.Rev.D, 71, 3515
- [62] Shen, Y., et al., 2007, AJ, 133, 2222
- [63] Sheth, R.K. & Tormen, G., 1999, MNRAS, 308, 119
- [64] Sheth, R.K., Mo, H.J., Tormen, G., 2001, MNRAS, 323, 1
- [65] Siegel, E.R., et al., 2005, MNRAS, 356, 1117
- [66] Spergel, D. N., et al., 2003, ApJS, 148, 175
- [67] Spergel, D.N., et al. 2007, ApJS, 170, 377
- [68] Sugiyama, N., 1995, ApJS, 100, 281
- [69] Tegmark, M., et al., 2004, Phys.Rev.D., 69, 3501
- [70] Terlevich, R., Melnick, J., 1981, MNRAS, 195, 839
- [71] Tonry, et al. , 2003, ApJ, 594, 1
- [72] Vikhlinin, A. & Forman, W., 1995, ApJ, 455, 109
- [73] Yang, Y., Mushotzky, R.F., Barger, A.J., Cowie, L.L., Sanders, D.B., Steffen, A.T., 2003, ApJ, 585, L85
- [74] Yang, Y., Mushotzky, R.F., Barger, A.J., Cowie, L.L., 2006, ApJ, 645, 68
- [75] Wang, Y. & Mukherjee, P., 2006, ApJ, 650, 1
- [76] Wei, H., 2008, European Phys.J. C, 60, 449
- [77] Wood-Vasey W.M., et al., 2007, ApJ, 666, 694